



**HAL**  
open science

## Design and parameter tuning of a robust model predictive controller for UAVs

Nathan Michel, Sylvain Bertrand, Giorgio Valmorbida, Sorin Olaru, Didier  
Dumur

► **To cite this version:**

Nathan Michel, Sylvain Bertrand, Giorgio Valmorbida, Sorin Olaru, Didier Dumur. Design and parameter tuning of a robust model predictive controller for UAVs. IFAC 2017 - 20th World Congress of the International Federation of Automatic Control, Jul 2017, Toulouse, France. hal-02009890

**HAL Id: hal-02009890**

**<https://hal.science/hal-02009890v1>**

Submitted on 6 Feb 2019

**HAL** is a multi-disciplinary open access archive for the deposit and dissemination of scientific research documents, whether they are published or not. The documents may come from teaching and research institutions in France or abroad, or from public or private research centers.

L'archive ouverte pluridisciplinaire **HAL**, est destinée au dépôt et à la diffusion de documents scientifiques de niveau recherche, publiés ou non, émanant des établissements d'enseignement et de recherche français ou étrangers, des laboratoires publics ou privés.

# Design and parameter tuning of a robust model predictive controller for UAVs

Nathan Michel<sup>\*,\*\*</sup> Sylvain Bertrand<sup>\*</sup> Giorgio Valmorbida<sup>\*\*</sup>  
Sorin Olaru<sup>\*\*</sup> Didier Dumur<sup>\*\*</sup>

<sup>\*</sup> ONERA - The French Aerospace Lab, F-91123 Palaiseau, France  
(e-mail: nathan.michel@onera.fr ; sylvain.bertrand@onera.fr)

<sup>\*\*</sup> L2S, CentraleSupélec, CNRS, Univ. Paris-Sud, Université  
Paris-Saclay, 3 rue Joliot-Curie, Gif-Sur-Yvette 91192, France  
(e-mail: giorgio.valmorbida@l2s.centralesupelec.fr ;  
sorin.olaru@l2s.centralesupelec.fr ; didier.dumur@centralesupelec.fr)

---

**Abstract:** Two formulations of model predictive control (MPC) that have robustness properties over conventional MPC are presented and studied for the control of the translational dynamics of an Unmanned Aerial Vehicle (UAV). These controllers are using results from invariant sets theory. Their tuning is studied, and their performances are compared in simulations in a context of bounded additive disturbance.

*Keywords:* Robust MPC, UAV, bounded additive disturbance, polytope, parameters tuning

---

## 1. INTRODUCTION

The last decade has witnessed a significant increase on the number of tasks performed by Unmanned Aerial Vehicles (UAVs). Among these we can cite commercial tasks such as goods delivery (Mo et al. (2016)), terrain mapping (Tahar et al. (2011)) and building facade assessment (Choi and Kim (2015)). The design of controllers enabling UAVs to perform autonomously such tasks should take into account safety and technological constraints, such as distance to obstacles or actuator limitations. Moreover, UAVs are subject to disturbances such as ground effect or aerodynamic perturbations when flying close to walls or rigid obstacles (McKinnon (2015)).

Previous work has been carried out on robust control of UAVs, from a switching model strategy (Alexis et al. (2011)) to a robust PID controller (Kada and Ghazzawi (2011)). These strategies are designed to guarantee robustness with respect to bounded disturbances, but suffer either from constraints limitation or from a computational aspect.

In this context, the constraint handling by the control law can benefit from Model Predictive Control strategies. Also, the ability to handle bounded disturbances on the system dynamics has been extensively studied and current MPC strategies allow for improved robustness and stability properties (Scokaert and Mayne (1998) Langson et al. (2004)). Developments on the computational aspects of the solution to the associated optimization problem make MPC controllers possible candidate for embedded systems (Necoara et al. (2014) Harja et al. (2013)).

One possible robustification of a MPC strategy that does not increase much the optimization problem complexity consists in computing a trajectory for a disturbance free version of the system by a classical MPC, while simultaneously an additional control law maintains the state of the

perturbed system inside a “tube” around the nominal trajectory (Langson et al. (2004)). This method requires an a priori knowledge of the disturbance bounds that can affect the system to ensure the uncertain system remains in the “tube”. These strategies have been extensively studied for linear systems (Mayne et al. (2006) Mayne et al. (2005)). The problem of position stabilization of an UAV can fit into this framework.

The MPC controllers in this study are based on invariant sets (Blanchini (1999)), that are computed here using the method presented in (Olaru et al. (2010)). Closed loop stability is guaranteed for these controllers by making use of a terminal stabilizing constraint (Mayne et al. (2000)), defined by sets whose construction are detailed in this paper. The tuning of two linear robust MPC controllers (Mayne et al. (2005)) and a comparison of their performances are studied in simulations. The disturbance model used in simulations are based on results from McKinnon (2015).

This paper is structured as follow: In Section 2, the equations of motion of a quadrotor UAV are introduced while results on invariant sets and related properties are presented in Section 3. In Section 4, two robust MPC controllers are described, and their tuning is studied in Section 5. Simulation results are presented in Section 6.

*Notations* Given two sets  $X \in \mathbb{R}^n$  and  $Y \in \mathbb{R}^n$ , the Minkowski sum and Pontryagin difference are defined as:

$$X \oplus Y = \{x + y | x \in X, y \in Y\}$$
$$X \ominus Y = \{x | x \oplus Y \subset X\}$$

For two vectors  $x \in \mathbb{R}^3$  and  $y \in \mathbb{R}^3$ , the cross product is denoted as  $x \times y$ .

A polytope  $P$  can be described as the convex-hull of a finite set of points  $\{v_1, v_2, \dots, v_{v(P)}\}$ ,  $P = \{x | x =$

$\sum_{i=1}^{v(P)} \lambda_i v_i, \sum_{i=1}^{v(P)} \lambda_i = 1\}$ , or as the set of solutions to a system of linear inequalities  $P = \{x|A(P)x + b(P) \leq 0\}$ .

## 2. UAV MODELING

Considering an inertial frame  $\mathbb{I} = (O, i, j, k)$  and a body frame  $\mathbb{B}$  attached to the vehicle, the UAV equations of motion are

$$\dot{\xi} = v \quad (1)$$

$$m\dot{v} = -mgk + RF + F_{ext} \quad (2)$$

$$\dot{R} = RQ(\omega) \quad (3)$$

$$J\dot{\omega} = -\omega \times J\omega + \tau \quad (4)$$

where  $\xi = (p_x, p_y, p_z)^\top$  is the position of the quadrotor in  $\mathbb{I}$ ,  $v = (v_x, v_y, v_z)^\top$  its velocity in  $\mathbb{I}$ ,  $m$  its mass,  $R \in SO(3)$  the orientation matrix,  $\omega = (\omega_x, \omega_y, \omega_z)^\top$  its angular velocity in the body frame,  $J$  its inertia matrix,  $g$  the gravity constant, and

$$Q(\omega) = \begin{pmatrix} 0 & -\omega_3 & \omega_2 \\ \omega_3 & 0 & -\omega_1 \\ -\omega_2 & \omega_1 & 0 \end{pmatrix}$$

The resulting force and torque generated by the quadrotor propellers are denoted  $F$  and  $\tau$  in the body frame  $\mathbb{B}$ .  $F_{ext}$  represents additional forces in the inertial frame due to external disturbance.

The following section will present an MPC strategy for the position regulation of the UAV (translational motion, i.e. (1) and (2)). Define

$$u = -gk + R_{ref}F_{ref}/m$$

yielding

$$\dot{v} = u + 1/m((RF - R_{ref}F_{ref}) + F_{ext}) \quad (5)$$

The design of an attitude controller, via the torque  $\tau$ , that guarantees the convergence of  $R$ , the actual orientation matrix, to  $R_{ref}$  the reference orientation matrix, is not discussed in this paper. Nevertheless, it is accounted for in the definition of the bounds in the disturbance term. The motors' dynamic is also neglected, thus  $F$  is assumed to converge instantaneously to  $F_{ref}$ . The equations (1) and (5) correspond to 3 double integrators with a bounded additive disturbance. We discretize them with a zero-order hold on  $u$  with sampling-time  $\delta_t$  to obtain

$$x[k+1] = Ax[k] + Bu[k] + w[k]$$

$$A = \begin{pmatrix} 1 & \delta_t & 0 & 0 & 0 & 0 \\ 0 & 1 & 0 & 0 & 0 & 0 \\ 0 & 0 & 1 & \delta_t & 0 & 0 \\ 0 & 0 & 0 & 1 & 0 & 0 \\ 0 & 0 & 0 & 0 & 1 & \delta_t \\ 0 & 0 & 0 & 0 & 0 & 1 \end{pmatrix}; B = \begin{pmatrix} \frac{\delta_t^2}{2} & \delta_t & 0 & 0 & 0 & 0 \\ 0 & 0 & \frac{\delta_t^2}{2} & \delta_t & 0 & 0 \\ 0 & 0 & 0 & 0 & \frac{\delta_t^2}{2} & \delta_t \end{pmatrix}^\top$$

where  $x = (p_x, v_x, p_y, v_y, p_z, v_z)^\top$ , and  $w \in \mathbb{W}$  is the discretized term obtained from the discretization of the disturbance  $1/m((R_{ref}F_{ref} - RF) + F_{ext})$ . If  $u$  is bounded and if the attitude controller is stabilizing, it can be shown that the error term  $R_{ref}F_{ref} - RF$  is also bounded. Since  $F_{ext}$  is assumed to be bounded too, then the disturbance term  $w$  can be considered as bounded. This system will be referred to as the *uncertain system*.

## 3. INVARIANT SETS AND FEEDBACK POLICY

The spatial and control constraints are defined by  $x \in \mathbb{X} \subset \mathbb{R}^6$  and  $u \in \mathbb{U} \subset \mathbb{R}^3$ ,  $\mathbb{X}$  and  $\mathbb{U}$  bounded polytopes

containing the origin in their interior. We also consider  $\mathbb{W}$  as a polytopic set containing the origin and bounding the discretized disturbance  $w$ . Denote the disturbance-free system

$$\bar{x}[k+1] = A\bar{x}[k] + B\bar{u}[k], \quad (6)$$

This system is called the *nominal system*. Let us consider the following feedback law for the uncertain system

$$u[k] = \bar{u}[k] + K(x[k] - \bar{x}[k]) \quad (7)$$

with  $K \in \mathbb{R}^{3 \times 6}$  a linear stabilizing state feedback gain such that  $A_K = A + BK$  is Schur. The difference, or error,  $z[k]$  between the state of the uncertain system  $x[k]$  and the nominal state  $\bar{x}[k]$  verifies:

$$z[k+1] = A_K z[k] + w[k] \quad (8)$$

*Definition 1.* (Blanchini (1999)) The set  $Z$  is said robustly positively invariant for the system (8) if for all  $z[k] \in Z$  and all  $w \in \mathbb{W}$ ,  $z[k+1] \in Z$ .

The following proposition states that the feedback law (7) ensures that the difference between the uncertain and the nominal state remains in a RPI set  $Z$ .

*Proposition 1.* (Mayne et al. (2005)) Suppose  $Z$  is RPI for  $z[k+1] = A_K z[k] + w[k]$ . Assume that  $x[k] \in \{\bar{x}[k]\} \oplus Z$  and  $u[k] = \bar{u}[k] + K(x[k] - \bar{x}[k])$ , then  $x[k+1] \in \{\bar{x}[k+1]\} \oplus Z$  for all  $w \in \mathbb{W}$ .

Define the sets

$$\bar{\mathbb{X}} = \mathbb{X} \oplus Z \quad (9)$$

$$\bar{\mathbb{U}} = \mathbb{U} \oplus KZ \quad (10)$$

If the nominal system satisfies the constraints ( $\bar{x} \in \bar{\mathbb{X}}$  and  $\bar{u} \in \bar{\mathbb{U}}$ ), then the uncertain system constraints are satisfied (i.e.  $x \in \mathbb{X}$  and  $u \in \mathbb{U}$ ).

**Remark:** it is mandatory to have  $Z \subset \mathbb{X}$  and  $KZ \subset \mathbb{U}$  to have non-empty feasible sets.

## 4. ROBUST MPC

### 4.1 Robust model predictive controller

This section presents the design of the nominal system control law using a MPC approach. The model predictive controller presented here is based on the solution of an optimal control problem  $P_N(\bar{x}[k])$  whose cost function

$$V_N(\bar{x}_0, \bar{\mathbf{u}}) = \sum_{i=0}^{N-1} (\bar{x}_i^t Q \bar{x}_i + \bar{u}_i^t P \bar{u}_i) + \bar{x}_N^t Q_f \bar{x}_N$$

is quadratic.  $P_N(\bar{x}[k])$  consists in minimizing the value function  $V_N(\bar{x}_0, \mathbf{u})$  with  $\bar{x}_0$  the current state of the nominal system  $\bar{x}[k]$ . In this optimization problem, the control input sequence  $\bar{\mathbf{u}} = (\bar{u}_0, \bar{u}_1, \dots, \bar{u}_{N-1})$  is the sole decision variable.

$$P_N(\bar{x}[k]) : V_N^0(\bar{x}[k]) = \min(V_N(\bar{x}_0, \bar{\mathbf{u}}))$$

$$\bar{u}_i \in \bar{\mathbb{U}}, \forall i \in \{0, \dots, N-1\}$$

$$\bar{x}_0 = \bar{x}[k]$$

$$\bar{x}_i \in \bar{\mathbb{X}}, \forall i \in \{0, \dots, N-1\}$$

$$\bar{x}_N \in \bar{\mathbb{X}}_f \subset \bar{\mathbb{X}}$$

With  $\bar{x}_{i+1} = A\bar{x}_i + B\bar{u}_i$  for all  $i \in \{0, \dots, N-1\}$  as dynamical constraints. The optimal control sequence is denoted  $\bar{\mathbf{u}}^0$ . The weighting matrices  $Q$ ,  $P$  and  $Q_f$  are positive definite.  $N$  is the prediction horizon. The terminal

cost  $Q_f$  and the terminal set  $\bar{\mathbb{X}}_f$  are defined to ensure stability.

*Proposition 2.* (Mayne et al. (2005)) Let  $k_f \in \mathbb{R}^{3 \times 6}$  be a feedback gain matrix. Suppose  $k_f$ ,  $Q_f$  and  $\bar{\mathbb{X}}_f$  are such that:

$$\begin{aligned} (A + Bk_f)\bar{\mathbb{X}}_f &\subset \bar{\mathbb{X}}_f \\ k_f\bar{\mathbb{X}}_f &\subset \bar{\mathbb{U}} \end{aligned} \quad (11)$$

$$\begin{aligned} \bar{\mathbb{X}}_f &\subset \bar{\mathbb{X}} \\ ((A + Bk_f)\bar{x})^t Q_f (A + Bk_f)\bar{x} + k_f \bar{x}^t P k_f \bar{x} \\ - \bar{x}^t Q_f \bar{x} &\leq 0, \forall \bar{x} \in \bar{\mathbb{X}}_f \end{aligned} \quad (12)$$

Then the origin is exponentially stable for the controlled nominal system and recursive feasibility of the optimization problems is ensured.

The feasibility domain of the optimization problem  $P_N(\bar{x})$  is denoted  $\bar{\mathbb{X}}_N$ . Once the optimization problem  $P_N(\bar{x}[k])$  is solved, the nominal control input  $\bar{u}[k]$  is set as the first element of the optimal control input sequence  $\bar{\mathbf{u}}_0^0$ . The next nominal state  $\bar{x}[k+1]$  and the control input  $u[k]$  is given by Equation (7).

The successive optimization problems can be precomputed: they involve the nominal state only, which is not impacted by the disturbance sequence. It is possible to compute the nominal system trajectory offline before the flight while the component  $K(x[k] - \bar{x}[k])$  ensures the uncertain system remains in a "tube" centered on this trajectory.

#### 4.2 An alternative version

The control input sequence  $\mathbf{u}$  is the only decision variable of the optimization problem  $P_N(\bar{x}[k])$  previously described. The change presented here, as initially proposed in Mayne et al. (2005) consists in letting  $\bar{x}_0$  be a decision parameter of an optimization problem  $P'_N(x[k])$ . At each time step, the nominal state  $\bar{x}[k]$  and the optimal control sequence  $\bar{\mathbf{u}}^0$  are taken as the minimizer of the value function:

$$\begin{aligned} P'_N(x[k]) : V_N^0(x[k]) &= \min(V_N(\bar{x}_0, \bar{\mathbf{u}})) \\ \bar{u}_i &\in \bar{\mathbb{U}}, \forall i \in \{0, \dots, N-1\} \\ x[k] &\in \{\bar{x}_0\} \oplus Z \\ \bar{x}_i &\in \bar{\mathbb{X}}, \forall i \in \{0, \dots, N-1\} \\ \bar{x}_N &\in \bar{\mathbb{X}}_f \subset \bar{\mathbb{X}} \end{aligned}$$

With  $\bar{x}_{i+1} = A\bar{x}_i + B\bar{u}_i$  for all  $i \in \{0, \dots, N-1\}$ . The optimal control sequence is denoted  $\bar{\mathbf{u}}^0$  and the optimal initial state  $\bar{x}_0^0$ . The control is

$$u[k] = \bar{\mathbf{u}}_0^0 + K(x[k] - \bar{x}_0^0)$$

The feasibility domain of the optimization problem  $P'_N(x[k])$  is denoted  $\bar{\mathbb{X}}_N$ . It can be proved that  $\bar{\mathbb{X}}_N \oplus Z = \bar{\mathbb{X}}_N$  (Mayne et al. (2005)). The conditions on  $Q_f$  and  $\bar{\mathbb{X}}_f$  defined in Proposition 2 guarantee recursive feasibility and robust exponential stability of the set  $Z$  for the controlled uncertain system.

The successive optimization problems involved in this controller can not be solved offline, indeed, the disturbance  $w[k]$  can not be forecast and it impacts the state  $x[k+1]$ . Therefore, the optimization problems have to be solved

online.

An interesting property of this controller is the following: *Proposition 3.*  $\forall x \in Z$ ,  $V_N^0(x) = 0$ ,  $\bar{x}_0^0 = 0$ ,  $\bar{\mathbf{u}}^0 = \mathbf{0}$  and  $u = \bar{u} + K(x - \bar{x}) = Kx$

Once the uncertain system has reached the RPI set  $Z$ , the optimization problem is trivial and  $Z$  is invariant for the uncertain system.

Both controllers presented in this section have robustness properties with regards to bounded additive disturbance. The tuning of their parameters is studied in the next section, and their closed loop performances are compared in Section 6.

## 5. TUNING PARAMETERS

The impact of the weighting matrices  $Q$  and  $P$  and of the prediction horizon  $N$  of  $P_N(\bar{x})$  and  $P'_N(x)$  are not detailed here. These controllers involve two sets of tuning parameters:  $(K, Z)$  and  $(k_f, Q_f, \bar{\mathbb{X}}_f)$ .

### 5.1 Feedback gain $K$

The set  $Z$  defines the maximal distance  $z = x - \bar{x}$  between the nominal and the uncertain state, and can be considered as the key element of the control law regarding the precision of the controlled system with regards to the disturbance  $\mathbb{W}$ . Moreover, it also defines the constraints  $\bar{\mathbb{X}}$  and  $\bar{\mathbb{U}}$  of the optimization problems:

- a larger set  $Z$  implies a smaller set  $\bar{\mathbb{X}} = \mathbb{X} - Z$ .
- for a given feedback gain  $K$ , a larger set  $Z$  implies a smaller set  $\bar{\mathbb{U}} = \mathbb{U} - KZ$

For a given feedback gain  $K$ , it is possible to define the minimal Robust Positive Invariant (mRPI) set  $Z^*$  Blanchini (1999)

$$Z^* = \bigoplus_{i=0}^{\infty} A_K^i W$$

With  $A_K^i$  being the matrix  $A_K$  to the  $i^{\text{th}}$  power, and  $\bigoplus$  the Minkowski sum. A feedback gain  $K$  leading to larger eigenvalues of  $A_K$  will result in a smaller set  $Z^*$  and a larger set  $KZ^*$ . In terms of optimal problems constraints:

- Larger eigenvalues lead to a larger feasible MPC set  $\bar{\mathbb{X}} = \mathbb{X} - Z^*$
- Larger eigenvalues lead to a smaller feasible control set  $\bar{\mathbb{U}} = \mathbb{U} - KZ^*$

Hence, the tuning of  $K$  impacts both the disturbance rejection and the constraints of the optimization problems.

**Remark:** In general,  $Z^*$  is not a polytope and cannot be explicitly characterized. In practical, the set  $Z$  is chosen as being an RPI outer approximation of the mRPI  $Z^*$ .

### 5.2 Feedback gain $k_f$

The admissible initial condition set  $\bar{\mathbb{X}}_N$  is deduced from the terminal constraints set  $\bar{\mathbb{X}}_f$ . The admissible initial condition sets for different horizon length  $i \in \{1, \dots, N\}$  are given by the following relations

$$\begin{aligned} \bar{\mathbb{X}}_1 &= \{\bar{x} \in \bar{\mathbb{X}} | \exists \bar{u} \in \bar{\mathbb{U}}, A\bar{x} + B\bar{u} \in \bar{\mathbb{X}}_f\} \\ \bar{\mathbb{X}}_{i+1} &= \{\bar{x} \in \bar{\mathbb{X}} | \exists \bar{u} \in \bar{\mathbb{U}}, A\bar{x} + B\bar{u} \in \bar{\mathbb{X}}_i\} \forall i \in \{1, \dots, N-1\} \end{aligned}$$

A larger set  $\bar{\mathbb{X}}_f$  leads to larger sets  $\bar{\mathbb{X}}_N$  of admissible initial conditions for a horizon prediction of  $N$ . The set  $\bar{\mathbb{X}}_f$  has

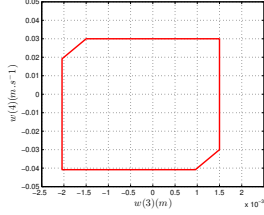


Fig. 1. Projection of the disturbance set on  $(p_y, v_y)$ .

to verify (11). A smaller feedback gain  $k_f$  leads to a larger set  $\bar{\mathbb{X}}_f$ , hence to a larger set  $\bar{\mathbb{X}}_N$ .

**Remark:** Due to (12), the feedback gain  $k_f$  has an impact on the terminal state cost  $Q_f$ .

## 6. SIMULATIONS

Consider below the example related to a critical flight of the UAV close to a wall. The state constraints are  $x \in \mathbb{X} = \{x | -5m \leq p_x \leq 5m, -0.5m \leq p_y \leq 1m, -0.2m \leq p_z \leq 1m, -1m.s^{-1} \leq v_x, v_y, v_z \leq 1m.s^{-1}\}$ . The control input constraints are  $u \in \mathbb{U} = \{u | -1m.s^{-2} \leq u_x, u_y, u_z \leq 1m.s^{-2}\}$ . The structure of the above constraints are such that the three directions  $(p_x, v_x)$ ,  $(p_y, v_y)$  and  $(p_z, v_z)$  can be addressed independently. Hence, the 6 dimensional optimization problem is separated into 3 independent 2-dimensional optimization problems. In the following, the results will be presented for one direction  $y$ . Similar results are obtained in the other two directions.

The weighting matrices  $R$  and  $Q$  are  $R = 0.1I_3$  and  $Q = \text{diag}(10, 1, 10, 1, 10, 1)$ . The sampling-time is  $\delta_t = 0.1s$  and the horizon length  $N = 15$ . The disturbance  $w$  is modeled as the sum of two components:

- the external force  $w_{ext}$  due to the proximity of a wall, whose value is taken from the models in McKinnon (2015) obtained by experimentations,
- a bounded disturbance term  $w_{ran}$ , whose value is randomly chosen in a set  $\mathbb{W}_{ran}$  at each time step

The projection of the set  $\mathbb{W}$  is presented in Figure 1.

### 6.1 Feedback controller $K$

The feedback gain  $K$  is computed using a pole placement strategy for the matrix  $A_K$ . The method presented in Olaru et al. (2010) defines, for a given feedback gain  $K$ , a sequence of RPI sets  $\mathbf{Z} = (Z_0, Z_1, \dots)$ . These sets are presented in Figure 2 for the set of poles  $\{0.70, 0.60\}$  regarding the direction  $y$ . The iterations increase the complexity of the polytope while decreasing its area (Figure 2).  $Z$  is chosen as  $Z_6$  in this simulation.

The set  $Z_6$  is presented for three sets of poles  $\{0.30, 0.20\}$ ,  $\{0.70, 0.60\}$  and  $\{0.90, 0.80\}$ . The associated bounds on  $\bar{u}$  are  $|\bar{u}| \leq 0.34, 0.54$  and  $0.59m.s^{-2}$ . A set of poles closer to 0 tends to increase the size of  $\bar{\mathbb{X}}$  while reducing the size of the set  $\bar{\mathbb{U}}$ .

The simulation is run with the set of poles  $\{0.70, 0.60\}$  for  $A_K$ .

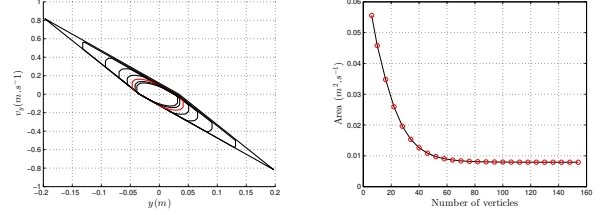


Fig. 2. (Left) Projection of the different sets  $Z_i, i = 0, \dots, 8$  on  $(p_y, v_y)$  for the following set of poles  $\{0.70, 0.60\}$ . (Right) Relation between the area of the iterations  $Z_i$  and their number of vertices  $v(Z_i)$ .

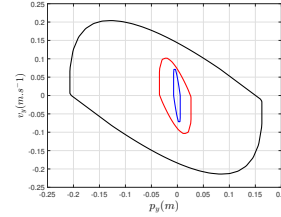


Fig. 3.  $Z_6$  for three different sets of poles:  $\{0.30, 0.20\}$  (blue),  $\{0.70, 0.60\}$  (red) and  $\{0.90, 0.80\}$  (black).

### 6.2 Terminal constraints

The feedback gain  $k_f$  is computed using a pole placement strategy for the matrix  $A + Bk_f$ . In this study, the algorithm used to compute the set  $\bar{\mathbb{X}}_f$  is the following

- Initialization:  $\Omega_0 = \{x \in \bar{\mathbb{X}} | k_f x \in \bar{\mathbb{U}}\}$
- Iteration:  $\Omega_{i+1} = \{x | A(\Omega_i)x + b(\Omega_i) \leq 0, A(\Omega_i)(A + Bk_f)x + b(\Omega_i) \leq 0\}, \forall i \leq 0$

The computation stops at the  $l^{th}$  iteration such that  $\Omega_{l+1} = \Omega_l$ , which implies  $(A + Bk_f)\Omega_l \subset \Omega_l$ . Thus, the set  $\Omega_l$  verifies the conditions of Proposition 2. Finite convergence of the algorithm is not guaranteed with the above strict stopping criterion. However, a relative convergence test can be used based on the decrease of the Hausdorff distance between consecutive iterations. It can be noted that the convergence speed increases for smaller eigenvalues of  $A + Bk_f$  which is relative to the contraction factor of the set mapping.

Figure 4 presents the sets  $\bar{\mathbb{X}}_f$  and  $\bar{\mathbb{X}}_N$  obtained for different sets of poles of  $A + Bk_f$ . Poles closer to 1 increase the size of the set of admissible initial conditions while increasing the complexity of the set  $\bar{\mathbb{X}}_f$ , that defines constraints of the optimization problem. The simulation is run with the set of poles  $\{0.95, 0.90\}$  for  $A + Bk_f$ .

### 6.3 Controller performance comparison

Both controllers have been simulated with the same admissible initial conditions  $x[0] = (0.5, 0, 0.5, 0, 0.5, 0)^T$  and random disturbance sequence  $w_{ran}$ . The stabilization problem consists in steering the state of the system to the reference chosen to be the origin. The closed-loop performances regarding  $p_y$  are illustrated in Figure 5, and the control input in Figure 6.

The control input is closer to saturation ( $u_y = 1m.s^{-2}$ ) for controller 2. This is due to the fact that  $x - \bar{x}$  takes

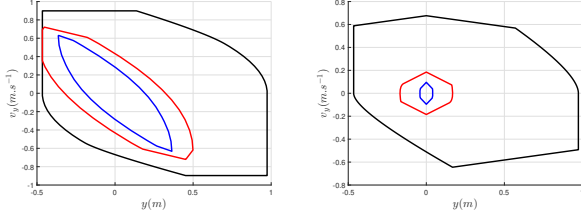


Fig. 4. Projection of the sets  $\bar{X}_f$  (left) and  $\bar{X}_N$  (right) on  $(p_y, v_y)$  for three sets of poles:  $\{97, 95\}$  (black),  $\{90, 80\}$  (red) and  $\{80, 60\}$  (blue).

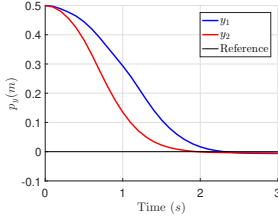


Fig. 5. Time evolution of  $y$  for both controllers.

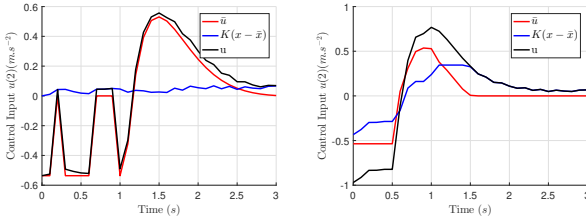


Fig. 6. Time evolution of the control input  $u$ ,  $\bar{u}$  and  $K(x - \bar{x})$  with controller 1 (left) and controller 2 (right).

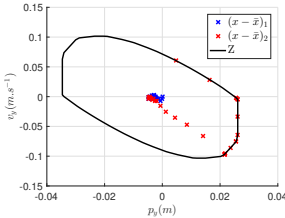


Fig. 7. Projection on the plane  $(p_y, v_y)$  of the difference  $x - \bar{x}$  with controller 1 (blue) and controller 2 (red).

extremal values in  $Z$  for controller 2 (Figure 7). Moreover, Figure 6 illustrates that  $\bar{u}$  and  $K(x - \bar{x})$  have the same sign until  $\bar{u} = 0$  (i.e. once the uncertain system has reached the set  $Z$  as mentioned in Proposition 3). This version allows the "tube" control input  $K(x - \bar{x})$  to not only reject disturbance but also to contribute in steering the state of the uncertain system to the reference.

In both simulations, the state of the uncertain system  $x$  remains in the "tube"  $\bar{x} \oplus Z$  as illustrated in Figure 7.

## 7. CONCLUSION

We have presented the computation of the sets involved in the robust model predictive controller presented in Mayne et al. (2005) for a simplified UAV model. The tuning parameters and their impact on both the system performance and the optimization problem have been

studied. Two robust model predictive controllers have been compared in simulations, using disturbance models from McKinnon (2015).

## REFERENCES

- Alexis, K., Nikolakopoulos, G., and Tzes, A. (2011). Switching model predictive attitude control for a quadrotor helicopter subject to atmospheric disturbances. *Control Engineering Practice*, 19(10), 1195 – 1207.
- Blanchini, F. (1999). Set invariance in control. *Automatica*, 35(11), 1747 – 1767.
- Choi, S. and Kim, E. (2015). Building crack inspection using small uav. In *2015 17th International Conference on Advanced Communication Technology (ICACT)*, 235–238.
- Harja, G., Hernandez, A., Keyser, R.D., and Nascu, I. (2013). Embedded real-time mpc implementation using rapid prototyping tools: A thermal process case study. In *2013 17th International Conference on System Theory, Control and Computing (ICSTCC)*, 250–255.
- Kada, B. and Ghazzawi, Y. (2011). Robust pid control design for an uav flight control system. In *World Congress on Engineering and Computer Science*, volume 2.
- Langson, W., Chrysochoos, I., Raković, S., and Mayne, D. (2004). Robust model predictive control using tubes. *Automatica*, 40(1), 125 – 133.
- Mayne, D., Raković, S., Findeisen, R., and Allgöwer, F. (2006). Robust output feedback model predictive control of constrained linear systems. *Automatica*, 42(7), 1217 – 1222.
- Mayne, D., Rawlings, J., Rao, C., and Scokaert, P. (2000). Constrained model predictive control: Stability and optimality. *Automatica*, 36(6), 789 – 814.
- Mayne, D., Seron, M., and Raković, S. (2005). Robust model predictive control of constrained linear systems with bounded disturbances. *Automatica*, 41(2), 219 – 224.
- McKinnon, C.D. (2015). *Data Driven, Force Based Interaction for Quadrotors*. Ph.D. thesis, University of Toronto.
- Mo, R., Geng, Q., and Lu, X. (2016). Study on control method of a rotor uav transportation with slung-load. In *2016 35th Chinese Control Conference (CCC)*, 3274–3279.
- Necoara, I., Stoican, F., Clipici, D., Patrascu, A., and Hovd, M. (2014). A linear mpc algorithm for embedded systems with computational complexity guarantees. In *2014 18th International Conference on System Theory, Control and Computing (ICSTCC)*, 363–368.
- Olaru, S., De Doná, J., Seron, M., and Stoican, F. (2010). Positive invariant sets for fault tolerant multisensor control schemes. *International Journal of Control*, 83(12), 2622–2640.
- Scokaert, P.O.M. and Mayne, D.Q. (1998). Min-max feedback model predictive control for constrained linear systems. *IEEE Transactions on Automatic Control*, 43(8), 1136–1142.
- Tahar, K.N., Ahmad, A., and Akib, W.A.A.W.M. (2011). Uav-based stereo vision for photogrammetric survey in aerial terrain mapping. In *2011 IEEE International Conference on Computer Applications and Industrial Electronics (ICCAIE)*, 443–447.